Journal of Nuclear Materials 204 (1993) 124–130
North-Holland

journal of nuclear materials

Metal fuel test program in the FFTF

A.L. Pitner and R.B. Baker
Westinghouse Hanford Company, P.O. Box 1970, Richland, WA 99352, USA

Irradiation testing of metal fuel assemblies in the Fast Flux Test Facility (FFTF) has demonstrated the viability of this robust fuel design for liquid metal reactor applications. This fuel design provides high burnup capability with reduced fabrication costs relative to standard mixed-oxide FFTF driver fuel assemblies. Development of this fuel design required the establishment of innovative sodium bonding technology as well as special techniques for sodium bond quality verification. Eight metal fuel test assemblies have been irradiated under demanding conditions to burnups as high as 143 MWd/kgM with no indication of pin breach. The unique FFTF instrumentation system has permitted the in situ observation of axial fuel growth in metal fuel assemblies.

1. Introduction

Eight separate liquid metal reactor (LMR) test assemblies containing metal (U–Zr and U–Pu–Zr) fuel pins have been irradiated in the Fast Flux Test Facility (FFTF) to burnup levels as high as 143 MWd/kgM. The first metal fuel test irradiated in the FFTF was designated IFR-1. This was an Argonne National Laboratory (ANL) test to support the Integral Fast Reactor (IFR) and the U.S. Department of Energy (DOE) Advanced Metal Fuel Reactor (ALMR) concepts. The MFF-1 and MFF-1A tests followed and each contained a mixture of binary (U–Zr) metal fuel pins, uranium dioxide (UO_2) fuel pins, and mixed oxide (MOX) UO_2–PuO_2 fuel pins.

In the late 1980s a plan was developed to convert the FFTF core from MOX-fueled drivers to metal-fueled drivers. This latter fuel design, designated Series III.b, capitalized on recent advancements in material and fuel development to provide a robust and economical LMR fuel concept with high power and high burnup capabilities. High pin power (i.e., nominal peak of 56 kW/m or 17 kW/ft) operation is permitted by the good thermal conductivity of metal fuel and the sodium bonding between the fuel and cladding. The use of near-zero swelling ferritic-martensitic HT9 alloy for duct, cladding, and wire-wrap material; increased fission gas plenum volume; and past ANL metal fuel concepts [1] permit high burnup levels (i.e., 150 MWd/kgM after 900 equivalent full power days [EFPD]) to be attained. The most recent phase of metal fuel testing in the FFTF was directed toward qualification of this metal-fueled driver fuel assembly (DFA) [2]. Two prototype (MFF-2 and MFF-3) and three Series III.b qualification tests (MFF-4, MFF-5, and MFF-6) were fabricated and irradiated in the FFTF to support this design qualification.

Experimental results from this testing series also provide data for the ALMR being designed by the General Electric Company for the DOE. The reference ALMR fuel design employs HT9 alloy for duct, cladding, and wire wrap material, and sodium bonded U–Pu–Zr metal fuel pins.

2. Fuel assembly design and fabrication

This section describes the fuel pin and assembly design used for metal fuel irradiations in the FFTF. A description of the various fuel pin designs is presented first. Because the Series III.b fuel design is the design proposed for a metallic driver fuel in the FFTF, that design is discussed in greater detail. A discussion of the sodium bonding technology developed for this program is also included.

2.1. Various metal fuel pin designs

All metal fuel pins that have been irradiated in the FFTF are 2.4 m (8 ft) in length and have a fuel column length of 91.4 cm (36 in.) with 6.86 mm (0.270 in.) diameter cladding. The IFR-1 test used 20 percent cold-worked D9, a titanium-modified austenitic stainless steel, and the remaining tests all used HT9

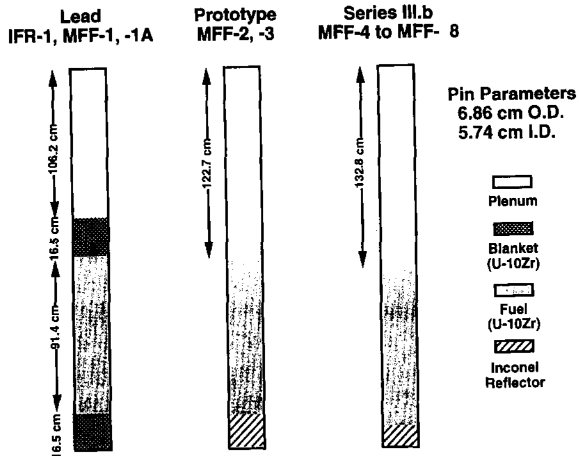

Fig. 1. Evolution of pin design in FFTF testing program.

cladding. The IFR-1 test contained both binary (U–10wt%Zr) and ternary (U–8wt%Pu–10wt%Zr and U–19wt%Pu–10wt%Zr) fuel pins. The MFF-1 and MFF-1A tests each contained a mixture of binary metal fuel pins, UO_2 fuel pins, and MOX fuel pins. All other test assemblies in the MFF series contained only binary fuel. All metal fuel pins in these tests used sodium between the fuel and cladding as a thermal bond.

Differing design characteristics of the pins tested are shown schematically in fig. 1. The early test pins (IFR-1, MFF-1, and MFF-1A) contained 16.5-cm- (6.5-in.-) long axial blankets of depleted U–10wt%Zr on each end of the fuel column. The MFF-2 and MFF-3 prototype tests employed no axial blankets. A 16.5-cm-(6.5-in.-) long neutron reflector was located only at the bottom of the fuel column, thereby increasing the pin gas plenum length by 16.5 cm (6.5 in.). The Series III.b qualification tests (MFF-4 and on) used only a 6.4-cm-(2.5-in.-) long reflector at the bottom, providing an additional 10-cm (4-in.) increase in the plenum length. The balance of the required reflector material is provided in the redesigned shield/orifice assembly.

2.2. *FFTF Series III.b fuel design*

The Series III.b fuel assembly design is shown schematically in fig. 2. The 169-fuel pin bundle assembly is contained in an HT9 duct tube. Use of this nonswelling duct material minimizes core distortion problems encountered with other alloys that swell under irradiation [3]. The duct tube is mechanically fastened to the end components (shield/orifice assembly and handling socket) by three "washer-type" retainers on each end [2]. The retainers are inserted into drilled holes in the duct tube and are welded on the inside diameter to the end hardware. This coupling technique results in a compliant system of end components and duct tube, thereby simplifying fabrication compared to

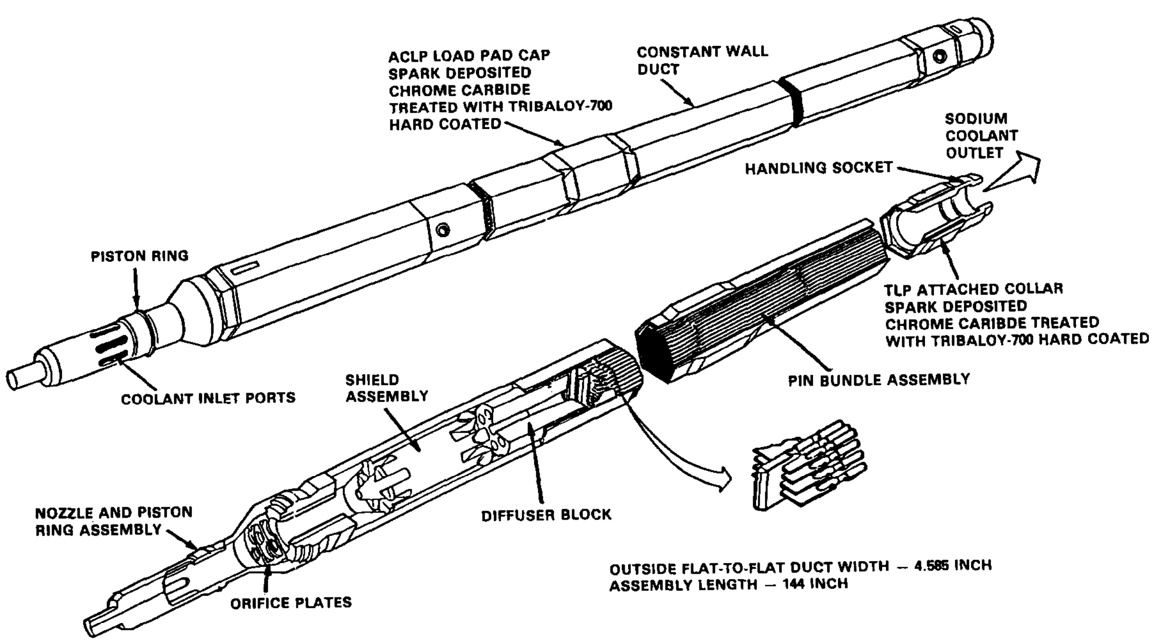

Fig. 2. FFTF Series III.b driver fuel assembly.

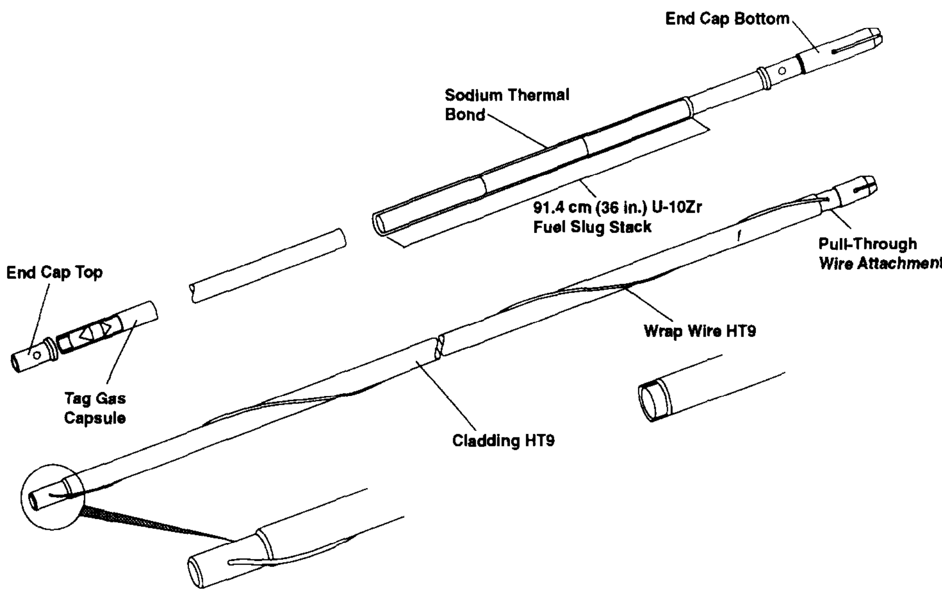

Fig. 3. FFTF metal fuel pin.

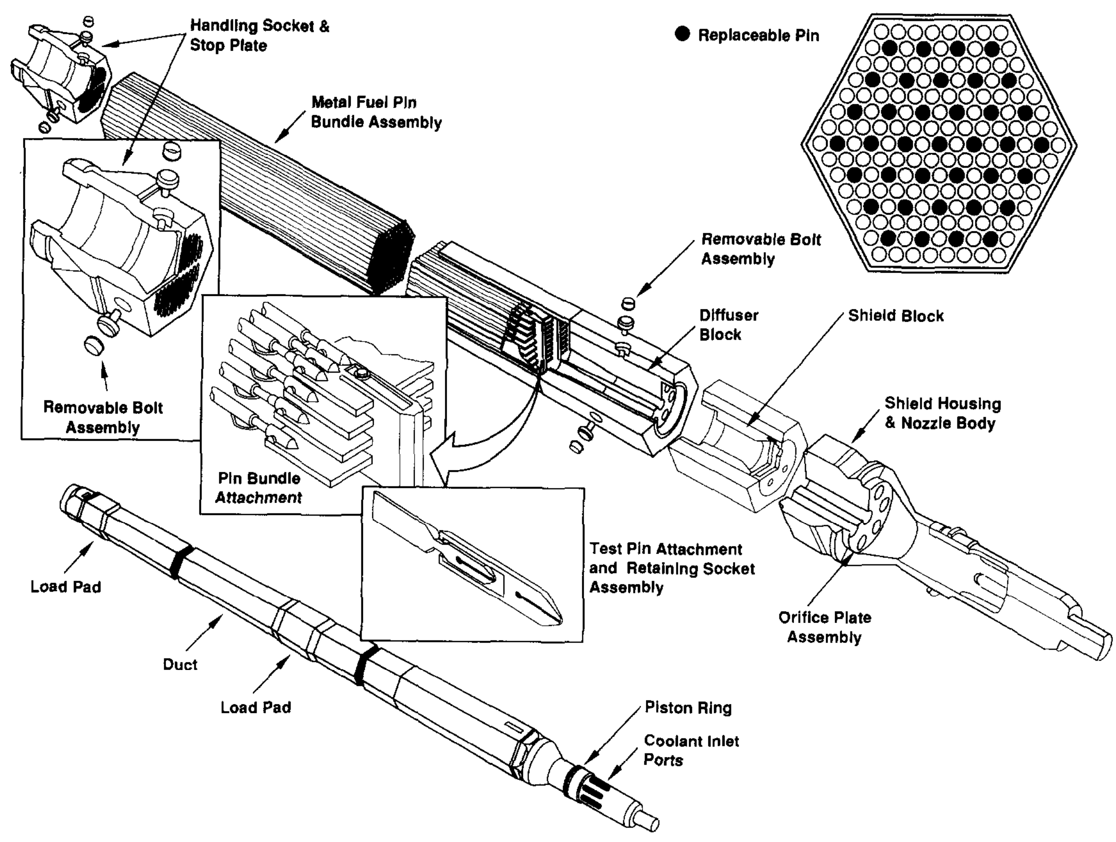

Fig. 4. MFF-8A reusable fuel test assembly.

the previously used circumferential butt welds to attach these components in FFTF DFAs. This also eliminates the need for elaborate measuring machines to characterize assembly straightness. A circumferential coolant flow restrictor is installed in a groove in the lower shield housing to limit sodium flow leakage between the duct tube and shield housing at this mechanical connection point. Because of the shorter handling socket associated with the improved Series III.b fuel pin design, the top portion of the duct tube is flared to form the load pad surface that interfaces with surrounding assemblies in the core. These modifications provided an improved FFTF fuel assembly design with no increase in cost.

A schematic of the Series III.b fuel pin design is presented in fig. 3. Two or three U-Zr metal fuel slugs make up the 91.4-cm- (36-in.-) long fuel column. The fuel smeared density is 75% theoretical density (TD), with a relatively large slug-to-cladding gap to accommodate the comparatively high swelling characteristics of metal fuel. The annular gap between fuel and cladding is filled with sodium to provide a good thermal bond. The gas plenum for the Series III.b fuel pin was extended by 10 cm (4 in.) relative to reference MOX driver fuel pins (i.e., Series I and II) to accommodate the increased gas release of this high burnup fuel. Each fuel pin contains a tag gas introduced by a capsule suspended from the top end cap, with a unique tag gas composition for each fuel assembly loaded in the core. Specific fuel pin parameters are summarized in table 1, which compares FFTF Series III.b (and MFF test pins) fuel pin parameters with those for the current ALMR fuel pin design.

One additional Series III.b qualification test was converted to a reusable test assembly [4], wherein up to 37 different test pins can be extracted and replaced after interim irradiation periods, and the test assembly returned to the FFTF for further irradiation. Further use of this modified assembly, designated MFF-8A and shown schematically in fig. 4, could provide flexible irradiation capabilities for fuel pin testing to high burnup levels with optional interim discharges to obtain data at staggered exposure levels.

Table 1
FFTF Series III.b and ALMR fuel pin parameters

	Series III.b (cm/in.)	US DOE ALMR (cm/in.)
Pins per assembly	169	331
Fuel height	91.4/36	134.6/53
Upper gas plenum height	132/52	188/74
Cladding material	HT9	HT9
Pin outer diameter	0.686/0.270	0.668/0.263
Cladding thickness	0.056/0.022	0.051/0.020
Fuel Slug diameter	0.498/0.196	0.490/0.193
Fuel-to-cladding bond	Sodium	Sodium
Fuel	U–Zr	U–Pu–Zr
Fuel smeared density (%TD)	75	75

The following outlines a number of significant economic advantages associated with the Series III.b fuel design.

(1) The fuel column in each pin is comprised of only two or three metal fuel slugs, compared to the many (~ 150) small pellets required to form the fuel column in typical MOX pins. This substantially reduces fuel fabrication costs. Also, plenum spacers and springs are not required in metal fuel pins. These features, combined with innovative fabrication techniques developed for metal fuel pins [5], expedite the overall pin assembly process.

(2) The high power capability of this metal fuel design permits the use of larger-diameter pins and a corresponding decrease in the number of pins required to form the fuel bundle assembly, while generating the same assembly power. The 169-pin bundle design represents a 22 percent decrease in pin count relative to the 217 pins loaded in the Series I and II FFTF MOX DFAs, thereby reducing overall pin fabrication costs and facilitating assembly operations.

(3) The design burnup capability of the Series III.b fuel is increased significantly over that of FFTF Series I and II DFAs (e.g., 150 MWd/kgM vs. 80 MWd/kgM). Accordingly, fuel supply needs are substantially reduced.

2.3. Sodium bonding technology

The large initial fuel slug-to-cladding gap required to accommodate the high swelling behavior of metal fuel is filled with sodium to provide a good thermal bond for heat transfer to maintain low fuel temperatures. Excessive voiding or porosity in the sodium bond could result in unacceptably high fuel temperatures during irradiation. Thus, it was necessary to develop and verify a sodium bonding technique that produced a product of suitable quality.

Loading of the sodium in the fuel pins is performed by encasing the sodium in a plastic sleeve, inserting the sleeve in the fuel pin cladding tube, and pneumatically injecting the sodium using a long hollow rod connected to an inert gas supply. The metal fuel slugs are loaded on top of the sodium column, and the fuel pins are then sealed and welded in a helium atmosphere. Set-

Table 2
Metal fuel tests irradiated in the FFTF

Test	Fuel [a]	Cladding	Peak linear power (kW/m–kW/ft)	Peak clad temp. (°C–°F)	Exp. EFPD	Peak burnup (MWd/kgM)	Fast fluence (10^{22} n/cm^2)
IFR-1	B & T	D9	49.2–15.0	604–1120	620	94	15.4
MFF-1A	B	HT9	42.7–13.0	577–1070	250	38	5.6
MFF-1	B	HT9	43.0–13.1	577–1070	685	95	17.3
MFF-2	B	HT9	54.1–16.5	618–1145	853	143	19.9
MFF-3	B	HT9	59.1–18.0	643–1190	726	138	19.2
MFF-4	B	HT9	56.8–17.3	618–1145	726	135	19.0
MFF-5	B	HT9	55.8–17.0	649–1200	503	101	14.0
MFF-6	B	HT9	55.8–17.0	588–1090	503	95	12.8
ALMR (Design)	T	HT9	31.5– 9.6	545–1013	~ 1400	141	33.0

[a] B = binary (U–Zr), T = ternary (U–Pu–Zr).

tling of the fuel slugs into the sodium bond is accomplished in the sodium bonding station, a unique tilting and vibrating tubular furnace with high throughput capability [5].

Sodium bond quality inspection employs both conventional radiography and eddy current testing. The radiography defines the sodium level in the fuel pin, which establishes the total porosity in the sodium bond based on the known sodium mass loading and annular volume between the fuel and cladding. The bond porosity distribution is determined by eddy current inspection. The general bond quality achieved by this bonding process, and the correlation between eddy current indications and actual porosity characteristics, were confirmed by examinations that entailed stripping the cladding from selected fuel pins to permit visual inspection [6]. Fuel pins that do not meet established sodium bond specifications are returned to the sodium

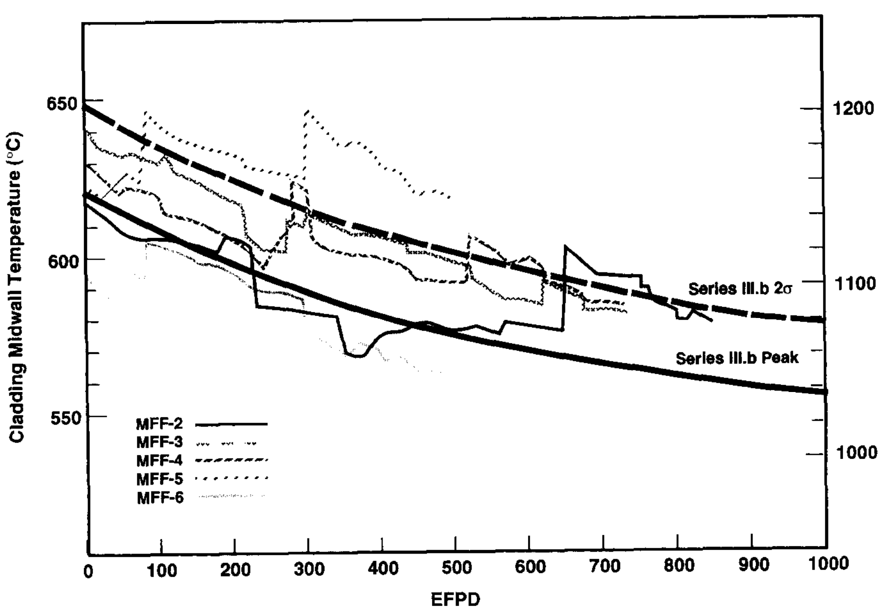

Fig. 5. FFTF metal fuel test temperatures.

bonding station for rework until acceptable bond quality is achieved.

3. Irradiation testing

3.1. Irradiation conditions

The irradiation conditions for the eight metal fuel tests irradiated in the FFTF through Cycle 12.B (March 1992) are summarized in table 2. Comparative design conditions for ALMR fuel assemblies are also included. Test conditions in several of these tests have been quite aggressive for HT9 cladding, but no fuel pin breaches have occurred. The cladding temperature histories of the recent MFF Series tests presented in fig. 5 further exemplify the aggressive nature of this testing. Projected peak nominal and two-sigma hot channel temperatures for the Series III.b fuel pins operating in the FFTF are included in the figure for reference.

The IFR-1 experiment is currently undergoing post-irradiation examination (PIE). The MFF-1 and MFF-1A tests have also been discharged from the reactor. The MFF-1A test assembly has been disassembled and pins are ready for PIE. The MFF-1 test is available for PIE. It was planned to discharge MFF-2 after 853 EFPD of exposure with burnup near 150 MWd/kgM, and continue the remaining four metal fueled tests as run-to-cladding-breach experiments to determine ultimate burnup capabilities of this fuel pin design. Actual disposition of the four tests remaining in the reactor after the most recent operation will depend on the final decision regarding future operation of the FFTF.

3.2. In situ observation of fuel growth

A relatively large radial gap is allowed in metal fuel pin designs to accommodate the known swelling characteristics of this fuel material [7]. It can be anticipated that there is an axial component of fuel growth associated with this swelling behavior. This growth was observed [8] in FFTF irradiations owing to the unique combination of a dimensionally stable FFTF oxide core and the calibrated proximity instrumentation present that continuously monitors individual assembly coolant outlet temperatures.

It was noted during the first several weeks of irradiation for metal fuel assemblies that measured coolant outlet temperatures dropped significantly more than would be projected based on fissile burnup effects. This observed decrease was interpreted as a drop in

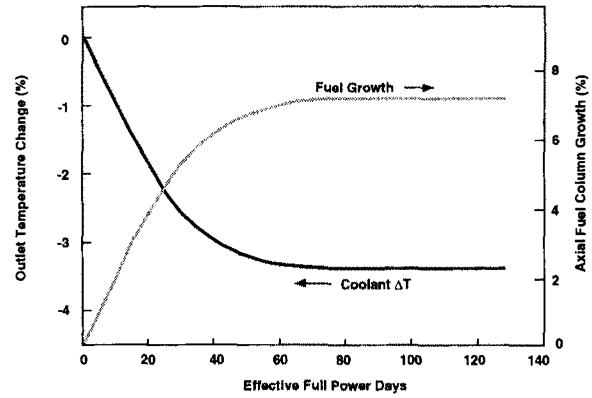

Fig. 6. Axial fuel growth effects observed in metal fuel test.

assembly power associated with the axial growth of the metal fuel column out of the active core region into the low-power region above the active core. As shown in fig. 6, the observed decrease in coolant temperature change through the assembly exceeded 3%. Based on a simple evaluation that assumed uniform fuel growth in the test assembly, the calculated axial fuel growth corresponding to this temperature decrease exceeded 7%, also shown in the figure. In absolute terms, the fuel columns expanded axially nearly 7 cm (2.6 in.). The fuel growth in the metal fuel assemblies appears to saturate after about 60 days of irradiation in the FFTF, or around a burnup of 1.5 at%. PIE can be used to verify axial fuel growth magnitudes, as well as characterize fuel and sodium bond performance, cladding strain behavior, fuel-cladding mechanical interaction, and other irradiation performance attributes.

4. Conclusions

Aggressive irradiation testing of metal fuel assemblies containing long fuel pins (similar to full-scale LMRs) has been successfully conducted in the FFTF, with no cladding breaches observed up to burnups approaching 150 MWd/kgM. The FFTF Series III.b DFA design (developed for this work) offers significant economic advantages over other FFTF DFA designs. In addition, quantitative estimates delineating the time dependence and magnitude of axial fuel swelling have been acquired through the unique FFTF test instrumentation system. The results of this work support the design development of the IFR fuel system, the design of the ALMR, and provide a potential advanced driver fuel system for the FFTF.

References

[1] R.G. Pahl, D.L. Porter, D.C. Crawford and L.C. Walters, J. Nucl. Mater. 188 (1992) 3.

[2] R.B. Baker, F.E. Bard and J.L. Ethridge, Proc. LMR: A Decade of LMR Progress and Promise (American Nuclear Society, Washington D.C., 1990) p. 184.

[3] J.L. Ethridge, R.B. Baker, R.D. Leggett, A.L. Pitner and A.E. Waltar, Proc. LMR: A Decade of LMR Progress and Promise (American Nuclear Society, Washington D.C., 1990) p. 163.

[4] A.L. Pitner and J.O. Dittmer, Trans. Am. Nuc. Soc. (Boston, Masschusetts, 1992) p. 187.

[5] J.O. Dittmer, M.W. Benecke and L.V. Feigenbutz, Trans. Am. Nucl. Soc. (Atlanta, Georgia, 1989) p. 143.

[6] A.L. Pitner and J.O. Dittmer, Trans. Am. Nucl. Soc. (Atlanta, Georgia, 1989) p. 144.

[7] G.L. Hofman, R.G. Pahl, C.E. Lahm and D.L. Porter, Met. Trans. 21A (1990) 517.

[8] E.R. Cramer and A.L. Pitner, Trans. Am. Nuc. Soc. (San Francisco, California 1989) p. 306.